Dalton Transactions

ROYAL SOCIETY OF CHEMISTRY

COMMUNICATION

View Article Online
View Journal | View Issue

Check for updates

Cite this: *Dalton Trans.*, 2024, **53**, 5351

Received 10th January 2024,
Accepted 26th February 2024

DOI: 10.1039/d4dt00078a

rsc.li/dalton

Reaction of $Ph_2C(X)(CO_2H)$ (X = OH, NH_2) with $[VO(OR)_3]$ (R = Et, *n*Pr): structure, magnetic susceptibility and ROP capability†

Mollie A. Glenister,[a] Josef W. A. Frese,[a] Mark R. J. Elsegood,[a] Angelos B. Canaj,[b] Euan K. Brechin[b] and Carl Redshaw*[c]

Reaction of $[VO(OR)_3]$ (R = Et, *n*Pr) with 2,2′-diphenylglycine afforded the alkoxide-bridged dimers $\{[VO(OR)(\mu\text{-}OR)][Ph_2C(NH_2)(CO_2)]\}_2$, whereas use of benzilic acid, in the presence of alkali metals, afforded 16-membered metallocycles $\{V_8(O)_4M(OR)_8[Ph_2C(OH)(CO_2)]_{12}\}$ (M = <1 Na, K). For the ring systems, magnetic susceptibility data is consistent with mixed-valence vanadium with an average oxidation state of 3.5. The dimer and ring systems are capable of the ring opening polymerisation (ROP) of ε-caprolactone under N_2, air, or as melts affording mostly low to medium molecular weight cyclic and linear products.

Current interest in the development of new catalytic species capable of the production of biodegradable polymers *via* ring opening polymerization (ROP) remains high.[1] This is driven by the need to replace materials such as polyethylene, which still finds widespread use despite the difficulties associated with lack of decomposition in landfill sites.[2] Metal alkoxides are the preferred catalyst type for ROP and, if necessary, the alkoxide catalyst can be generated *in situ* by the addition of an external alcohol. The other ligands that complete the coordination environment at the metal can greatly affect both the catalytic activity of the system and the resultant polymer properties. In this respect, we and others have been scoping a variety of ligand types in combination with numerous different metal centres with a view to accessing highly active, controllable ROP systems. As part of our studies, we have recently reported the use of the acids $Ph_2C(X)(CO_2H)$, where X = OH or NH_2, *i.e.* benzilic acid and 2,2′-diphenylglycine. Our interest in the use of such acids stems from the presence of the motif $Ph_2C(X)$, which has been shown to impart high crystallinity on products.[3] New ROP catalysts based on titanium, lithium, zinc, aluminium, and rare-earth metals incorporating the motif $Ph_2C(X)$ were reported, together with a number of intriguing molecular structures.[4] Recently, for the group V metals, we have investigated the use of niobium and tantalum alkoxide precursors, which afforded tetranuclear complexes $[M_4(OEt)_8(L^1)_4(\mu\text{-}O)_2]$ in the case of benzilic acid (L^1H_2), and dinuclear complexes $[Nb_2(OEt)_4(L^2H_2)_4(\mu\text{-}O)]$ in the case 2,2′-diphenylglycine (L^2H_3).[5]

Herein, as part of an on-going programme investigating the use of earth-abundant metal catalysts, we have extended our studies using this motif to vanadium-based systems, and reacted each of the two $Ph_2C(X)$-containing acids with the vanadyl tris(alkoxides) $[VO(OR)_3]$ (R = Et, *n*Pr). For X = NH_2, the alkoxide-bridged dimers $\{[VO(OR)(\mu\text{-}OR)][Ph_2C(NH_2)(CO_2)]\}_2$ (R = Et, *n*Pr) are formed, whilst for X = OH, 16-membered mixed-valence metallocycles $\{V_8(O)_4M(OR)_8[Ph_2C(OH)(CO_2)]_{12}\}$ are formed incorporating eight vanadium centres (Chart 1). In the case of benzilic acid, the presence of small amounts a sodium or potassium salts further aided crystallization. We note that a ferric wheel $[Fe(OMe)_2(Ph_2C(OH)(CO_2))]_{12}$ derived from benzilic acid was reported by Raptopoulou *et al.*,[6] whilst McInnes *et al.* have reported the V(III) octanuclear cluster $[V_8(OEt)_8(OH)_4(O_2CPh)_{12}]$ *via* a solvothermal route.[7] ROP catalysts based on vanadium have already shown promise when using other ancillary ligand types,[8] and there is interest in the use of heterometallic and multinuclear complexes as catalysts for ROP.[9]

Reaction of the vanadyl trisalkoxides $[VO(OR)_3]$ (R = Et, *n*Pr) with 2,2′-diphenylglycine, $Ph_2C(NH_2)(CO_2H)$, in refluxing toluene afforded, following work-up (MeCN), the yellow crystalline solids $\{[VO(OR)(\mu\text{-}OR)][Ph_2C(NH_2)(CO_2)]\}_2$ (R = Et **1**, *n*Pr **2**) in moderate to good yield. In the IR spectrum, the peak at 986 cm^{-1} is assigned to $\nu V{=}O$. Both solids can be recrystallized from saturated acetonitrile solutions at 0 °C. The molecular structures of both complexes were determined, and were found to be similar alkoxide-bridged dimers. We will only discuss **2**·2MeCN here; for **1** see the ESI (Fig. S1 and S2†). In

[a]*Plastics Collaboratory, Chemistry, School of Natural Sciences, University of Hull, Cottingham Road, Hull, HU6 7RX, UK. E-mail: c.redshaw@hull.ac.uk*
[b]*EaStCHEM School of Chemistry, University of Edinburgh, Edinburgh, EH9 3FJ, UK*
[c]*Chemistry Department, Loughborough University, Loughborough, Leicestershire, LE11 3TU, UK*

† Electronic supplementary information (ESI) available: Synthetic details for **1**–**8**; alternative views of **1**–**8**; crystallographic and ROP data. CCDC 2320818–2320821 and 2320775–2320778. For ESI and crystallographic data in CIF or other electronic format see DOI: https://doi.org/10.1039/d4dt00078a

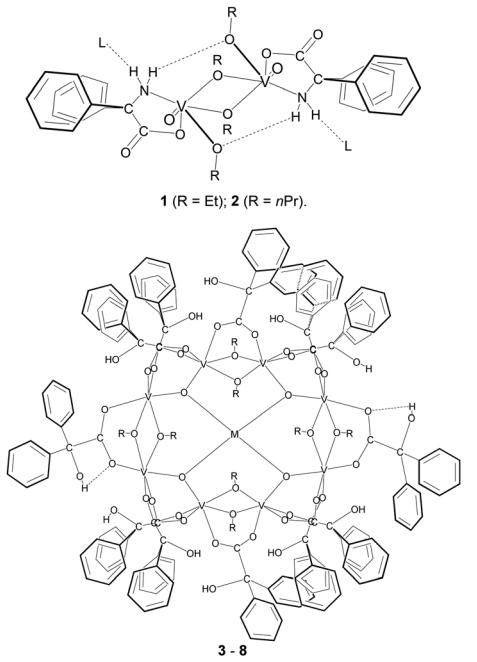

Chart 1 Complexes **1–8** prepared herein (**3**, R = *n*Pr, M = Na^+; **4**, R = Et, M = Na^+; **5**, R = *n*Pr, M = Na^+; **6** R = *n*Pr, M = Na^+; **7**, R = *n*Pr, M = K^+; **8** R = *n*Pr, M = K^+; L = NCMe). Note there is no L for **1**.

the case of **2**, the formula is $\{VO(On\text{-}Pr)(\mu\text{-}OnPr)[Ph_2C(NH_2)(CO_2)]\}_2\cdot 2(C_2H_3N)$, and there are two half molecules in the asymmetric unit. The molecule containing pseudo octahedral V(1) (Fig. 1) exhibits two intramolecular H-bonds N–H···O, plus two intermolecular H-bonds to MeCN molecules. The molecule containing pseudo octahedral V(2) (Fig. S3†) exhibits a different H-bonding pattern. While there is still the N–H···O intramolecular H-bond, the second N–H links to O(2) in the molecule containing V(1), not to an MeCN.

There are two unique MeCNs, *i.e.* two per V_2 complex. One unique MeCN is H-bonded to the molecule containing V(1), the other is not H-bonded. Molecules pack into 1D chains *via* the intermolecular H-bonds described above (Fig. S4, ESI†).

Reaction of two equivalents of $[VO(OnPr)_3]$ with benzilic acid (benzH) in refluxing toluene afforded, following work-up (MeCN), small dark prisms in low yield (<10%). A preliminary crystal structure determination unexpectedly revealed a large macrocyclic structure comprising eight vanadium centres and twelve benzilic acid-derived ligands (Fig. S5, ESI†). At the centre of the metallocycle was electron density suggestive of a sodium ion. This was thought to arise from the drying of the solvent toluene. However, the data associated with this structure, $\{V_8(O)_4Na_{0.75}(OnPr)_8[Ph_2C(OH)(CO_2)]_{12}\}\cdot 8MeCN$, **3**·8MeCN, was of rather poor quality (see Fig. S5 and Table S1, ESI†).

In order to try and improve both the yield and quality of the crystal data, we conducted the synthesis in the presence of a number of sodium and potassium salts. Indeed, from combinations of $[VO(OR)_3]$ (R = Et, *n*Pr), MI or MH (M = Na, K) and benzilic acid, we were able to isolate highly crystalline products in slightly higher yield (*ca.* 28–40%). The molecular structure of a representative example is shown in Fig. 2, with selected bond lengths and angles given in the caption; a view of the core is given in Fig. S9, ESI.† As for the preliminary structural data mentioned above, the product, namely $\{V_8(O)_4Na_{0.45}(OnPr)_8[Ph_2C(OH)(CO_2)]_{12}\}\cdot 6.38MeCN$ **5**·6.38MeCN, was a 12-membered

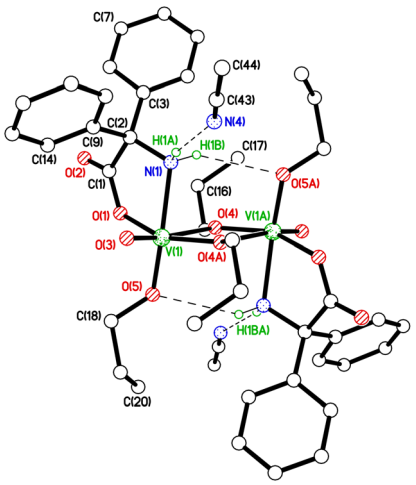

Fig. 1 Molecular structure of $\{VO(OnPr)(\mu\text{-}OnPr)[(Ph_2C(NH_2)CO_2)]\}_2\cdot 2MeCN$ (**2**·2MeCN). Selected bond lengths (Å) and angles (°): V(1)–O(1) 1.9559(10), V(1)–O(3) 1.5859(11), V(1)–O(4) 2.2993(10), V(1)–O(4A) 1.8484(9), V(1)–O(5) 1.7926(11), V(1)–N(1) 2.1845(12); V(1)–O(1)–C(1) 125.06(9), V(1)–N(1)–C(2) 112.73(8), V(1)–O(4)–V(1A) 107.46(4), O(4)–V(1)–O(4A) 72.54(4).

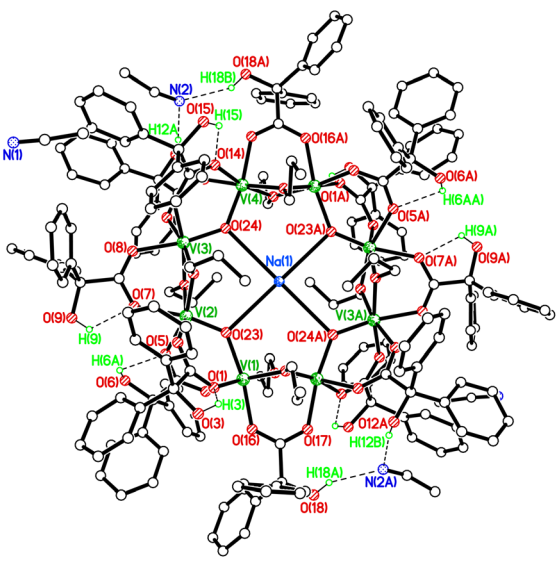

Fig. 2 Molecular structure of $\{V_8(O)_4Na_{0.45}(OnPr)_8[Ph_2C(OH)(CO_2)]_{12}\}\cdot 6.38MeCN$ (**5**·6.38MeCN). Selected bond lengths (Å) and angles (°): V(1)–O(1) 2.043(3), V(1)–O(4) 2.033(3), V(1)–O(16) 2.022(3), V(1)–O(19) 1.975(3), V(1)–O(20) 1.954(3), V(1)–O(23) 1.976(3), V(1)···V(2) 3.3749(9), Na(1)–O(23) 3.028(2), V(2)–O(2) 2.016(3), V(2)–O(5) 2.031(3), V(2)–O(7) 2.113(3), V(2)–O(21) 1.941(3), V(2)–O(22) 1.962(2), V(2)–O(23) 1.726(3), V(2)···V(3) 3.0068(9); V(1)–O(23)–V(2) 131.35(14), V(1)–O(20)–V(4A) 99.81(12), V(2)–O(23)–Na(1) 114.85(11).

metallocycle containing eight vanadium centres and twelve benzilic acid derived ligands. Furthermore, there is a central Na^+ ion, modelled as partially occupied 0.449(13) with the occupancy refined.

For **5**·6.38MeCN, the molecule lies on a centre of symmetry so half is unique. There was evidence of non-merohedral twinning, however no twin law could be determined. In all of the similar V_8 structures, it is presumed that the charge of the central, partially occupied, alkali metal ion is balanced by the loss of some benzilic acid O*H* hydrogens, probably disordered. In all cases, the O*H* atoms needed to be included in a constrained manner with either rotational freedom or aligned to make the most reliable H-bond. In terms of charge, the 28 negative charges (12 × $benz^{1-}$, 4 × oxo^{2-}, 8 × O*n*Pr^{1-}) suggest mixed-valence V, with a mean oxidation state of 3.5. The benzilic OH hydrogens generally make H-bonds with either adjacent carboxylate oxygens or nearby MeCN of crystallisation. V···V distances bridged by two alkoxides and one carboxylate are shorter than those bridged by two carboxylates and an oxo ligand.

This $\{V_8(O)_4M(OR)_8[Ph_2C(OH)(CO_2)]_{12}\}$ structural motif appears to be quite general for the various combinations of benzilic acid, MX, and $[VO(OR)_3]$, and the molecular structures of **4**, **6–8** are provided in the ESI (Fig. S7, S11, S13, S15;† note the quality of **6** is less good but structurally in accord with the others). A notable comparison with the behaviour showcased in the series is that of crown ethers which also possess cavities which bind to alkali metal ions.[10] When the cavity diameters are compared with the structures in this series (Fig. S17, ESI†), it can be seen that the V_8 rings have a larger diameter and are closer in size to 21-crown-7 (Table S2†). This crown ether configuration favours larger ions such as Rb^+ and Cs^+, therefore suggesting reasoning for the partial occupancy herein, *i.e.* the larger cavity of the V_8 structures is unfavourable to the smaller Na^+ and K^+ ions. We note that it has previously been reported that alkali metals can be used to control ring size.[11]

D*c* magnetic susceptibility measurements were performed on a polycrystalline sample of **5** over the temperature range T = 2–275 K, in an applied field (B) of 0.1 T (Fig. 3), where $\chi = M/B$, and M is the magnetisation. At 275 K, the χT value of 4.3 cm^3 K mol^{-1} is below the expected value for spin-only contributions to the susceptibility for a $[V_8]$ unit with an average oxidation state of 3.5 (5.5 cm^3 mol^{-1} K, g = 2.0). Upon cooling, the χT product decreases rapidly reaching a value of 0 cm^3 K mol^{-1} at 18 K. The data are therefore suggestive of the presence of very strong antiferromagnetic exchange between neighbouring vanadium ions and a diamagnetic ground state. A quantitative interpretation of the susceptibility data is hampered by the valence-delocalised nature of **5**. However, we note that the behaviour of **5** is similar to that of $[V_8(OEt)_8(OH)_4(O_2CPh)_{12}]$[8] and to vanadium dimers bridged by $[(O)(O_2CR)_2]$ and $[(OR)_2(O_2CR)]$ units, as in **5**, which are known to mediate strong antiferromagnetic exchange.[12] Similar behaviour is also observed in structurally related $[Fe_8]$ wheels with similar bridging units.[13]

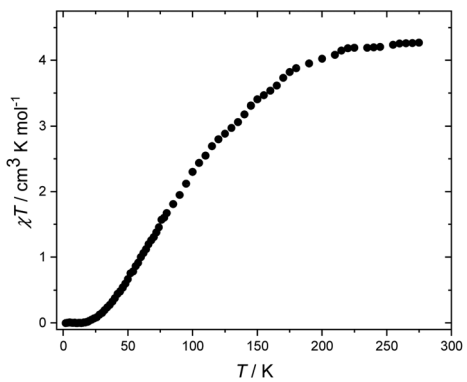

Fig. 3 Experimental χT *versus* T data for **5** measured in the T = 2–275 K temperature range in an applied field of B = 0.1 T.

Complexes **1**, **2**, **4**, and **8** have been screened for their potential to act catalysts for the ROP of ε-caprolactone (Table 1). Using **1**, the ratio [CL] : [**1**], time and temperature were all varied. At ambient temperature, and using a ratio of 500 : 1 ([CL] : [**1**]), no activity was observed. Increasing the temperature to 70 °C led to low conversion (*ca.* 15%), however on further raising the temperature to 130 °C, quantitative conversion was observed. Varying the ([CL] : [**1**]) proved to be detrimental with lower conversion and less control. Conducting the run under air also led to full conversion, albeit with less control and a lower molecular weight product. When conducted as a melt, a

Table 1 ROP of ε-CL catalysed by the complexes **1**, **2**, **4** and **8** [a]

Entry	Cat.	$[CL]_0 : [Cat]_0$	Conv.[b] (%)	M_n [c] (calc.)	M_n [d] (obs.)	$Đ$[e]
1[f]	**1**	500 : 1	0	—	—	—
2[g]	**1**	500 : 1	15.4	—	—	—
3	**1**	500 : 1	100	57 088	5890	1.58
4	**1**	250 : 1	18.4	5268	5130	1.76
5	**1**	1000 : 1	90.9	103 771	4650	2.60
6[h]	**1**	500 : 1	100	57 088	2415	1.75
7[i]	**1**	500 : 1	4.1	—	—	—
8[j]	**1**	500 : 1	87	49 669	3560	1.92
9[h,j]	**1**	500 : 1	35	19 993	3090	2.82
10	**2**	500 : 1	75.2	42 935	3680	1.42
11[h]	**2**	500 : 1	100	57 088	3330	2.03
12[j]	**2**	500 : 1	81.3	46 416	5370	1.84
13[h,j]	**2**	500 : 1	100	57 088	8600	3.25
14	**4**	500 : 1	50.5	28 838	2670	1.41
15[h]	**4**	500 : 1	100	57 088	3830	1.79
16[j]	**4**	500 : 1	88.5	50 525	6320	3.70
17[h,j]	**4**	500 : 1	65.8	37 570	2410	1.52
18	**8**	500 : 1	100	57 088	3430	3.64
19[h]	**8**	500 : 1	100	57 088	2070	1.82
20[j]	**8**	500 : 1	70.4	40 195	2550	1.81
21[h,j]	**8**	500 : 1	100	57 088	10 720	1.95

[a] Conducted at 130 °C under N_2 for 24 h unless otherwise stated; [catalyst] = 0.01 mmol. [b] Determined by ^{1}H NMR spectroscopy. [c] $M_{n(calc.)}$ = 114.14 × $[CL]_0/[cat]$ × %conv + $M_{end\ group}$. [d] $M_{n(obs)}$ and D obtained by GPC in THF relative to polystyrene standards corrected by the Mark–Houwink correction factor $M_{n(obs)} = M_{nGPC}$ raw data × 0.56. [e] Polydispersity index. [f] Conducted at 20 °C. [g] Conducted at 70 °C. [h] Conducted under air. [i] Conducted for 1 h. [j] Conducted as a melt (solvent-free conditions).

higher molecular weight product was formed with a conversion of *ca.* 80%. Complex **2** also exhibited full conversion when used either under air in solution or as a melt, affording in the latter case a higher molecular weight product (M_n 8600). For the V_8 complex **4**, the conversion at 130 °C under N_2 (entry 14) was half that observed for **1** (entry 3) and afforded a PCL polymer with half the molecular weight, albeit with slightly better control. A similar run under air (entry 15) led to quantitative conversion, whilst use of **4** as a melt (entry 16) also led to higher conversion (*ca.* 88%) and an increased molecular weight. However, the use of a melt under air (entry 17) led to a reduction in both the conversion (to *ca.* 66%) and molecular weight. Use of **8** at 130 °C in toluene under N_2 (entry 18) or air (entry 19) led to quantitative conversion, with higher molecular weight but less control for the former. Use of a melt in air (entry 21) proved more effective than a melt under N_2 (entry 20).

In nearly all cases, the molecular weights observed were significantly lower than the theoretical values, suggesting that transesterification had occurred. ^{1}H NMR spectra of the PCL formed indicated the presence of H-PCL-OH end groups (*e.g.*, Fig. S20, ESI†). However, from MALDI-ToF mass spectra (Fig. S21–S26, ESI†), it was evident that several PCL series were present (as sodium adducts). For **1** (entry 4, Table 1, Fig. S21†), these included chain polymers H-PCL-OH and the sodium exchange artefact, and a minor family with no end groups (cyclic) and the sodium exchange artefact. Similarly, for **1** as a melt (entry 9, Table 1, Fig. S22†), chain polymers H-PCL-OEt and the sodium exchange artefact and a minor cyclic family and the sodium exchange artefact. For **2** (entry 15, Table 1, Fig. S23†), the series with end groups H–/–OH was evident, whilst as a melt (entry 17, Table 1, Fig. S24†) at least two families were evident, including those with end groups HO–/–ONa and no end groups (cyclic). For **8** (entry 18, Table 1, Fig. S25†), at least three series of peaks were identified including the sodium exchange artefact for the PrO–/–H end group, the HO–/–H series, together with a number of lower intensity families *e.g.* MeO–/–H. Use of **8** as a melt under N_2 (entry 20, Table 1, Fig. S26†) afforded the PCL series HO–/–OH and the sodium exchange artefact, and PrO–/–H end groups. Use of other V-based complexes for the ROP of ε-CL has led to the isolation of multiple families of products with low to moderate molecular weight.[14]

Kinetic studies (Fig. S27–S30, ESI†), conducted using 500 : 1 ([CL]:[Cat]) revealed the rate trend **2** > **8** ≫ **4** > **1**, and this order is ascribed to the respective solubilities of the systems.

In conclusion, the reaction of the acids $Ph_2C(X)CO_2H$ with $[VO(OR)_3]$ led to very different products. In the case of X = NH_2, alkoxide bridged dimers were formed, whereas for X = OH, large macrocyclic structures of the type $\{V_8(O)_4M(OR)_8[Ph_2C(OH)(CO_2)]_{12}\}$ comprising eight vanadium centres, with average oxidation state of 3.5, and twelve benzilic acid derived ligands were isolated. The presence of an alkali metal cation (Na^+, K^+) favoured the formation of such macrocycles. The systems were capable of the ROP of ε-caprolactone, affording mixtures of low to medium molecular weight products ($M_n \leq 10\,720$) with differing or no end groups, and with varied control ($Đ$ 1.41–3.70).

Conflicts of interest

There are no conflicts to declare.

Acknowledgements

CR thanks the EPSRC (EP/S025537/1) for financial support. We thank the EPSRC National Crystallography Service, Southampton for data collection. The STFC are thanked for beam time at Daresbury Laboratory SRS. EKB, ABC thank The Leverhulme Trust (grant RPG-2021-176).

References

1 (*a*) Y. Sarazin and J.-F. Carpentier, *Chem. Rev.*, 2015, **115**, 3564–3614 and references therein; (*b*) C. Redshaw, *Catalysts*, 2017, **7**, 165–178; (*c*) J. Gao, D. Zhu, W. Zhang, G. A. Solan, Y. Ma and W.-H. Sun, *Inorg. Chem. Front.*, 2019, **6**, 2619–2652; (*d*) D. M. Lyubov, A. O. Tolpygin and A. A. Trifonov, *Coord. Chem. Rev.*, 2019, **392**, 83–145; (*e*) O. Santoro and C. Redshaw, *Catalysts*, 2020, **10**, 210; (*f*) O. Santoro, X. Zhang and C. Redshaw, *Catalysts*, 2020, **10**, 165–800.

2 L. W. McKeen, *Introduction to the use of Plastics in Food Packaging*, William Andrew Publishing, 2013, pp. 1–15; G. Manivasagam, A. Reddy, D. Sen, S. Nayak, M. T. Mathew and A. Rajamanikam, *Encyclopaedia of Biomedical Engineering*, ed. R. Narayan, Elsevier, Oxford, 2019, pp. 332–347.

3 M. Braun, *Angew. Chem.*, 1996, **108**, 565; M. Braun, *Angew. Chem. Int. Ed.*, 1996, **35**, 519–522.

4 Y. Al-Khafaji, M. R. J. Elsegood, J. W. A. Frese and C. Redshaw, *RSC Adv.*, 2017, **7**, 4510–4517; X. Wang, K.-Q. Zhao, S. Mo, Y. Al-Khafaji, T. J. Prior, M. R. J. Elsegood and C. Redshaw, *Eur. J. Inorg. Chem.*, 2017, 1951–1965; Y. F. Al-Khafaji, T. J. Prior, L. Horsburgh, M. R. J. Elsegood and C. Redshaw, *ChemistrySelect*, 2017, **2**, 759–768; J. Collins, O. Santoro, T. J. Prior, K. Chen and C. Redshaw, *J. Mol. Struct.*, 2021, **1224**, 129083; X. Zhang, T. J. Prior, K. Chen, O. Santoro and C. Redshaw, *Catalysts*, 2022, **12**, 935.

5 X. Zhang, T. J. Prior and C. Redshaw, *New J. Chem.*, 2022, **46**, 14146–14154.

6 C. P. Raptopoulou, V. Tangoulis and E. Devlin, *Angew. Chem., Int. Ed.*, 2002, **41**, 2386–3589.

7 R. H. Laye, M. Murrie, S. Ochsenbein, A. R. Bell, S. J. Teat, J. Raftery, H.-U. Güdel and E. J. L. McInnes, *Chem. – Eur. J.*, 2003, **9**, 6215–6220.

8 H. Ishikura, R. Neven, T. Lange, A. Galetová, B. Blom and D. Romano, *Inorg. Chim. Acta*, 2021, **515**, 120047.

9 (*a*) W. Gruszka and J. A. Garden, *Nat. Commun.*, 2021, **12**, 3252; (*b*) L.-J. Wo, W. Lee, P. K. Ganta, Y.-L. Chang, Y.-C. Chang and H.-Y. Chen, *Coord. Chem. Rev.*, 2023, **475**, 214847.

10 (*a*) R. D. Hancock, *J. Inclusion Phenom. Mol. Recognit. Chem.*, 1994, **17**, 63–80; (*b*) J. W. Steed, *Coord. Chem. Rev.*, 2001, **215**, 171–221.
11 R. W. Saalfrank, I. Bernt, E. Uller and F. Hampel, *Angew. Chem., Int. Ed. Engl.*, 1997, **36**, 2482–2485.
12 K. Kanamori, *Coord. Chem. Rev.*, 2003, **237**, 147–165.
13 C. Cañada-Vilalta, M. Pink and G. Christou, *Chem. Commun.*, 2003, 1240–1241.
14 See for example: M. R. J. Elsegood, W. Clegg and C. Redshaw, *Catalysts*, 2023, **13**, 998.